

Relative Distribution of Synapses in the A-Laminae of the Lateral Geniculate Nucleus of the Cat

SUSAN C. VAN HORN, ALEV ERIŞİR, AND S. MURRAY SHERMAN*

Department of Neurobiology, State University of New York,
Stony Brook, New York 11794-5230

ABSTRACT

Previous electron microscopic studies of synaptic terminal distributions in the lateral geniculate nucleus have been flawed by potential sampling biases favoring larger synapses. We have thus re-investigated this in the geniculate A-laminae of the cat with an algorithm to correct this sampling bias. We used serial reconstructions with the electron microscope to determine the size of each terminal and synaptic type. We observed that RL (retinal) terminals are largest, F (local, GABAergic, inhibitory) terminals are intermediate in size, and RS (cortical and brainstem) terminals are smallest. We also found that synapses from RL terminals are largest, and thus most oversampled, and we used synaptic size data to correct for sampling errors. Doing so, we found that the relative synaptic percentages overall are 11.7% for RL terminals, 27.5% for F, and 60.8% for RS. Furthermore, we distinguished between relay cells and interneurons with post-embedding immunocytochemistry for GABA (relay cells are GABA negative and interneurons are GABA positive). Onto relay cells, RL terminals contributed 7.1%, F terminals contributed 30.9%, and RS terminals contributed 62.0%. Onto interneurons, RL terminals contributed 48.7%, F terminals contributed 24.4%, and RS terminals contributed 26.9%. We also found that RL terminals included many more separate synaptic contact zones (9.1 ± 1.6) than did F terminals (2.6 ± 0.2) or RS terminals (1.02 ± 0.02). We used these data plus the calculation of overall percentages of each synaptic type to compute the relative percentage of each terminal type in the neuropil: RL terminals represent 1.8%, F terminals represent 14.5%, and RS terminals represent 83.7%. We argue that this relative synaptic paucity is typical for driver inputs (from retina), whereas modulator inputs (all others) require many more synapses to achieve their function. *J. Comp. Neurol.* 416:509–520, 2000. © 2000 Wiley-Liss, Inc.

Indexing terms: thalamus; synaptic terminals; relay cells; interneurons; sensory transmission

The lateral geniculate nucleus of the cat has been one of the most intensely studied regions of the brain. We now appreciate that this is no mere relay of retinal signals to cortex, but rather involves variable and dynamically controlled alterations in the extent and properties of the retinal signals that are relayed (reviewed in Sherman and Guillery, 1996; Sherman and Koch, 1998). To appreciate the neural basis of this dynamic relay process, we must have a still better understanding of geniculate cell and circuit properties. A starting point is to provide a fuller description with the electron microscope of the various synaptic contacts found in the geniculate neuropil.

Three major types of synaptic terminal have been described in the main, A-laminae of the cat's lateral

geniculate nucleus (Guillery, 1969a,b; Sherman and Guillery, 1996). One type, which we shall refer to as *RL* (see Terminology and identification section in Materials and Methods), is very large, has round vesicles, and forms asymmetric contacts; this derives from retina.

Grant sponsor: USPHS; Grant number: EY03038.

Alev Erişir's current address is: Center for Neural Sciences, New York University, 4 Washington Pl #1056, New York, NY 10003.

*Correspondence to: S.M. Sherman, Department of Neurobiology, State University of New York, Stony Brook, New York 11794-5230.
E-mail: s.sherman@sunysb.edu

Received 2 July 1999; Revised 11 October 1999; Accepted 13 October 1999

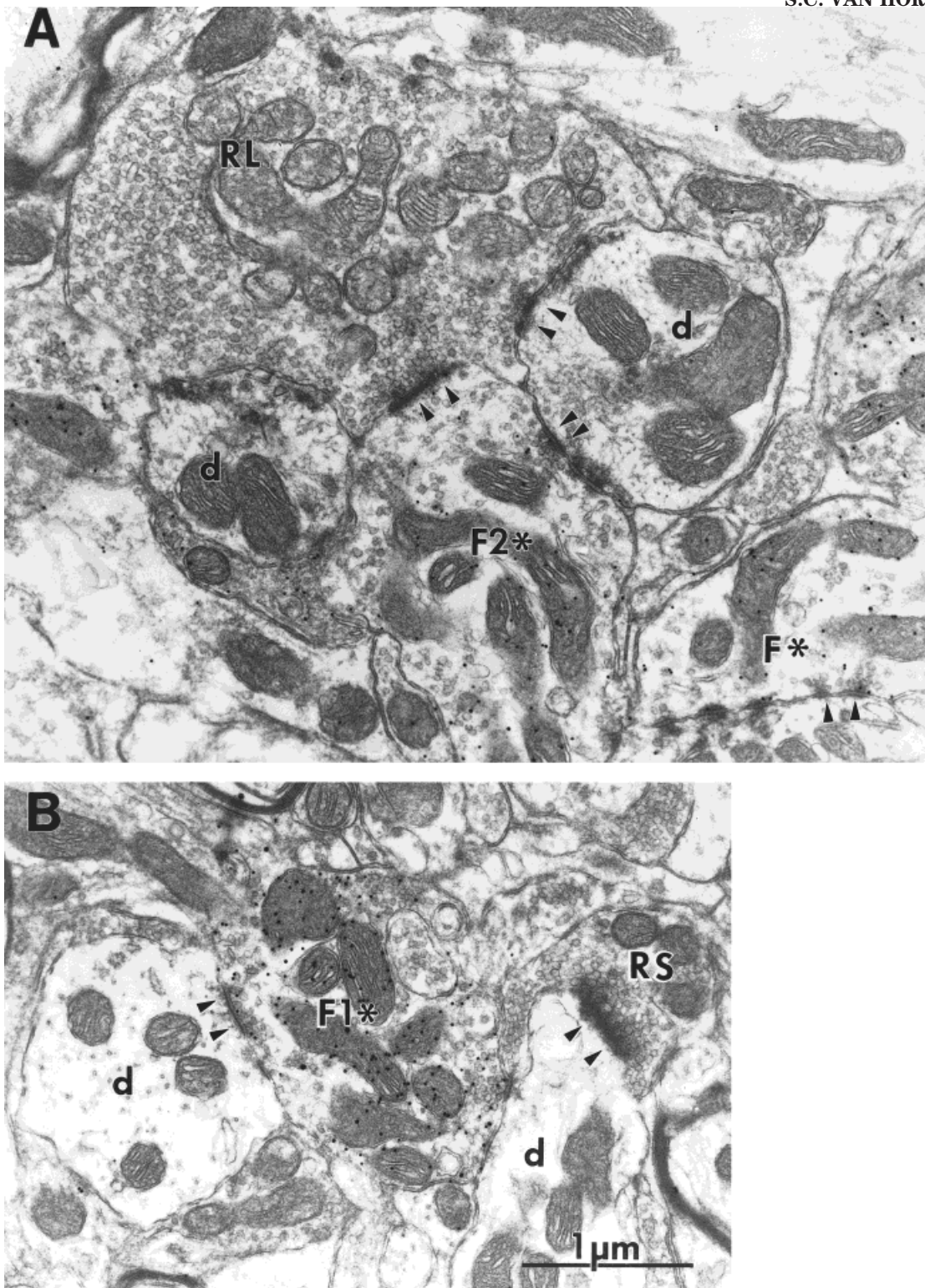


Fig. 1. Electron micrographs of identified terminal types in the A-laminae of the cat's lateral geniculate nucleus. The arrowheads indicate synaptic contacts, and the asterisks indicate GABA-positive (i.e., GABAergic) profiles, which are marked by the small black particles of the immunogold labeling for GABA. Examples of RL, F (including F1 and F2), and RS terminals are shown as well as dendritic profiles (d). The dendritic profiles in these views are all GABA negative, marking them as belonging to relay cells, and the F terminals are all GABA positive. RL terminals are GABA negative, display round and loosely packed vesicles, have pale mitochondria, and form asymmetric synaptic contacts. F terminals are GABA positive, display flat

or pleomorphic vesicles, and form symmetric synaptic contacts. RD terminals are GABA negative, display round and loosely packed vesicles, have dark mitochondria when present, and form asymmetric synaptic contacts. **A:** RL and F terminals. One of these is clearly an F2 terminal, because in the plane of section shown, it is both presynaptic and postsynaptic. The other F terminal is presynaptic only in this plane of section, and since serial sectioning was not done on it to check for the possibility that it might also be a postsynaptic target, thus identifying it as an F2 type. **B:** RS and F1 terminals. The F1 terminal was serially reconstructed (data not shown) to verify that it is strictly presynaptic. The scale bar in B also applies to A.

Another, much smaller type we refer to as *RS*¹ also has round vesicles and forms asymmetric contacts; this derives chiefly from cortex and brainstem. The third type, *F*, has flattened or pleomorphic vesicles and forms symmetric contacts; this type derives almost exclusively from local γ -aminobutyric acid (GABA)ergic cells—both intrageniculate interneurons and cells of the nearby thalamic reticular nucleus. This last type has been further subdivided into terminals arising from axons of these local GABAergic cells (*F1*) and terminals emanating from distal dendrites of interneurons (*F2*).

It is of obvious importance to determine the distribution of these various synaptic terminals and their relationship to relay cells and interneurons in the lateral geniculate nucleus. Several electron microscopic studies have provided estimates of the relative number of synaptic terminals in the geniculate neuropil, suggesting that the relative percentages of RL, RS, and F terminals are roughly 15–20%, 50–60%, and 20–30%, respectively (Guillery, 1969a; Wilson et al., 1984; Erişir et al., 1998). However, these studies have typically included all synaptic terminals encountered in single thin sections without dealing with possible sampling biases. We have shown in a study of the RS terminals that the size of the synaptic contact zone strongly biases the probability of detecting the terminal in most sampling strategies (Erişir et al., 1997). This is because the larger the contact zone, the more consecutive thin sections it will traverse, and thus the more likely any particular thin section will include the contact zone. Thus, by measuring the size of the synaptic zones with serial reconstruction, it is possible to correct for these biases, and we have used an algorithm here to do so. Also, by combining this with immunohistochemistry for GABA, we were able to distinguish between relay cell and interneuron targets of the various synapses and thus estimate the relative distribution of inputs for each cell type.

MATERIALS AND METHODS

We studied the brains of 11 adult cats using techniques that we have described previously (Wilson et al., 1984; Bickford et al., 1993; Erişir et al., 1997, 1998) and that are briefly outlined below. All animals were treated strictly in accordance with NIH guidelines for the care and use of laboratory animals, and the protocols used were approved by the Institutional Animal Care and Use Committee at the State University of New York at Stony Brook. Following deep barbiturate anesthesia, the cats were perfused transcardially with 2% paraformaldehyde and 2% glutaraldehyde or 4% paraformaldehyde and 0.2% glutaraldehyde. We postfixed the brains overnight with the same fixative and then cut them in the sagittal plane on a Leica VT 1000 S vibratome at 50–60 μ m. Sections through the lateral geniculate nucleus were trimmed to a selected area, osmicated in 2% osmium tetroxide in 0.1 M sodium phosphate buffer (PB) at pH 7.4, dehydrated in a graded series of ethyl alcohol, and treated with a 1:1, then a 3:1 mixture of resin (Durcupan ACM

Epoxy from Electron Microscopy Sciences, Fort Washington, PA) and 100% ethyl alcohol.

Sections were then vacuum infiltrated in pure resin overnight, flat embedded between two pieces of ACLAR (Ted Pella, Redding, CA), and placed in a 68°C oven for 48–72 hours. The embedded sections were blocked to include the A-laminae of the lateral geniculate nucleus and glued onto the end of a blank resin block. All the data presented here are taken from the A-laminae of the lateral geniculate nucleus. We cut serial ultrathin sections at approximately 80 nm on a Reichert-Jung Ultracut E ultramicrotome and placed these on Formvar-coated, nickel single-slot grids. All sections were counterstained with uranyl acetate and lead citrate to add contrast.

Every fifth or sixth section was immunostained for GABA with a postembedding procedure following a previously described protocol (Phend et al., 1992; Bickford et al., 1994). Briefly, sections were incubated in anti-GABA (Sigma, St. Louis, MO) primary antibody diluted 1:4000–1:5000 in a Tris-buffered saline solution with Triton X-100 (TBST), pH 7.6, rinsed, and followed by treatment in a gold-conjugated goat anti-rabbit IgG secondary diluted 1:25 (15nm: Amersham Life Sciences, Arlington Heights, IL) in TBST, pH 8.2.

We determined synapse and terminal sizes from serial reconstructions through these structures. We first photographed synaptic zones of the three main terminal types (RL, RS, and F) that showed clear synaptic areas at a scope magnification of $\times 12,000$ with a JEOL 1200 EXII electron microscope. A low-power micrograph ($\times 500$) was also taken of the areas, which enabled us to use landmarks such as blood vessels, somata, etc. to help locate the same terminal in adjacent sections. To keep track of all the synaptic zones within each terminal in an orderly fashion, it was critical to examine the ultrathin sections in the same orientation. For this purpose, the goniometer of the electron microscope proved to be useful to maintain a consistent orientation throughout the serial sections.

To identify RL, RS, and F terminals in the A-laminae of the lateral geniculate, we used four major criteria when examining the vesicle-filled profiles: 1) GABA content, 2) mitochondria contrast (pale or dark), 3) vesicle shape (round or pleomorphic), and 4) synaptic zone appearance (symmetrical or asymmetrical). The main discrimination between relay cells and interneurons was based on GABA immunoreactivity, since interneurons contain GABA and relay cells do not. The mitochondria contrast was used to discriminate between RL and RS terminals, although mitochondria could not always be recognized in RS terminals. F1 terminals, which derive from axons of interneurons and thalamic reticular cells, are strictly presynaptic, whereas F2 terminals, which derive from peripheral dendritic appendages of interneurons, are both pre- and postsynaptic. We could make this distinction with serial reconstructions through F terminals. Otherwise all GABAergic terminals are classified as F. For RS terminals, which include cortical and brainstem axons, no further classification is performed since morphological criteria alone are not sufficient for such classification.

From examination of the serial micrographs, we determined the terminal type, the number of synaptic zones each individual terminal displayed, the number of serial sections an individual synapse spanned, and its postsynaptic partner. When possible, depending on whether a glial sheath could be seen, we recorded whether a synaptic contact was made within or outside of a glomerulus.

¹ This varies slightly from previous terminology (e.g., Guillery, 1969a,b), which also included a "P" (i.e., "RLP") and "D" (i.e., "RSD") for "pale" and "dark" in reference to mitochondria. However, since mitochondria are often absent in RS terminals in single sections, we have abandoned the "P" and "D".

Three-dimensional reconstructions were made using HVEM 3-D (University of Colorado) and microVoxel (Indec Systems) systems.

Statistical analyses were performed by using non-parametric tests (Mann-Whitney, Chi-square, or Kruskal-Wallis).

RESULTS

The morphological criteria for differentiating terminal types in the lateral geniculate nucleus were sufficient to identify reliably GABA-containing F terminals (derived from local GABAergic cells), RL terminals (derived from retina), and RS terminals (derived almost exclusively either from cortex or from the parabrachial region of brainstem). Figure 1 illustrates typical examples. Figure 1A shows an RL terminal that is large and GABA negative and an F terminal that is small and GABA positive. Figure 1B shows another F terminal that is small and GABA positive along with an RS terminal that is small and GABA negative. The postsynaptic targets, usually dendrites, of identified terminals were also classified as belonging to relay cells, by being GABA negative (Fig. 1), or interneurons, by being GABA positive (Fig. 1A). Overall, we examined 208 synaptic zones from RL terminals, 159 from RS, and 120 from F.

We also serially reconstructed 14 RL, 15 RS, and 41 F (28 F1 type and 13 F2 type) terminals plus their synaptic zones. An example of these serial reconstructions is given in Figure 2. Figure 2A shows one of the thin sections of the series, with the F2 and RL terminals that were reconstructed, and Figure 2B,C shows the results of the reconstruction. It is worth noting that every one of these serially reconstructed terminals had at least one discernable synaptic contact zone; of course, such zones were frequently missed in many single sections.

Terminal sizes

From the serial reconstructions of complete terminals, we could determine the sizes of the different terminal types. Figure 3 summarizes these results in terms of the number of serial sections traversed by each terminal. As expected, RL terminals were the largest (spanning 55.6 ± 5.4 sections; here and below, the \pm values refer to the standard error of mean), F terminals next in average size (spanning 26.8 ± 1.4 sections), and RS terminals the smallest (spanning 15.9 ± 0.9 sections). These differences between any pairs of terminal were significant ($P \leq 0.001$). Within F terminals, we found no significant difference between the sizes of the F1 and F2 subtypes (for F1, 25.8 ± 1.5 sections; for F2, 28.9 ± 3.2 sections; $P > 0.1$).

Figure 4 shows for each serially reconstructed terminal the relationship between its actual volume and number of contacts formed. Note that the axes are scaled logarithmically. For the volume calculations, we measured the cross-sectional area of each terminal in each section and assumed a section thickness of 80 nm. The volumes of these terminals are as follows: for RL terminals, $9.58 \pm 1.29 \mu\text{m}^3$; for RS terminals, $0.39 \pm 0.05 \mu\text{m}^3$; for F1 terminals, $1.47 \pm 0.21 \mu\text{m}^3$; and for F2 terminals, $1.99 \pm 0.33 \mu\text{m}^3$. Except for the comparison between F1 and F2 terminals, which shows no statistically significant difference in size ($P > 0.1$), each pairwise comparison of these terminal types reveals a statistically significant difference ($P < 0.001$ for each comparison). It is interesting that RL and

RS terminals show no overlap in volume. This suggests that the larger RS terminals, which have been called "RLD" (for "round" vesicle, "large" profile, and "dark" mitochondria; Montero, 1991), either are small with respect to RL terminals or they are rare enough to be absent from our sample (see also Erişir et al., 1997).

Synaptic contact zones

Number of contact zones. Also from the serial reconstructions of complete terminals, we could determine the number of synaptic contacts formed by the terminals (Fig. 4). Typically, RS terminals contained a single synaptic zone. In contrast, RL and F terminals formed multiple contacts with several profiles. Examples of the synaptic relationships of three geniculate terminals in three-dimensional reconstructions are illustrated in Figure 2. RL terminals contained the most synaptic contact zones (9.1 ± 1.6), F terminals contained the next in number (2.6 ± 0.2), and RS terminals contained the fewest (1.02 ± 0.02). With one exception, these differences were statistically significant for each pairwise comparison ($P \leq 0.001$), including comparisons involving the F1 and F2 subsets of F terminals. The exception was the comparison between F1 and F2 terminals: synapses formed by F1 terminals (2.8 ± 0.3) were not significantly different in number from those formed by F2 terminals (2.2 ± 0.3 ; $P > 0.1$). It should be noted that, for F2 terminals, although we also found postsynaptic specializations on the terminals, the above counts refer only to synapses formed by F2 terminals onto other profiles, which were always GABA negative (i.e., relay cell) dendrites.

Figure 4 also shows a general and significant, positive relationship between the size of a terminal and number of contacts it forms. This is seen for the entire population of terminals ($r = +0.86$, $n = 70$, $P < 0.001$) as well as for the subsets of RL terminals ($r = 0.70$, $n = 14$, $P < 0.01$), F1 terminals ($r = +0.76$, $n = 28$, $P < 0.001$), and F2 terminals ($r = +0.82$, $n = 13$, $P < 0.001$). Only RS terminals showed no correlation ($r = +0.19$, $n = 15$, $P > 0.1$), possibly because, with one exception, these terminals formed only a single synapse.

Sizes of contact zones. The size of the contact zone for each terminal type was determined from the serial reconstructions through these zones as the number of consecutive sections that a morphologically identified synaptic zone traversed. We serially reconstructed many more synaptic zones than terminals, because the samples were selected mainly based on clear synapses rather than terminal bouton morphology, and only a subset of terminal boutons were photographed and reconstructed in their entirety. Basically, we started with a grid that was near the middle of a series, located in an area of lamina A and/or A1, and sampled every synapse we could clearly detect. We then photographed adjacent ultrathin sections preceding and following this middle section to allow serial reconstruction. Any new synapse or terminal encountered in this stack of photographs was included in the sampled until we reached the end of the series.

As noted below, this initial sampling procedure provided a sufficient number of synapses for reliable statistical analysis for all types studied with one exception: we initially sample only seven examples of synapses from RS terminals onto interneurons, and thus to increase the number of these synapses we went through our material a second time and selected only RS synapses onto interneurons until we

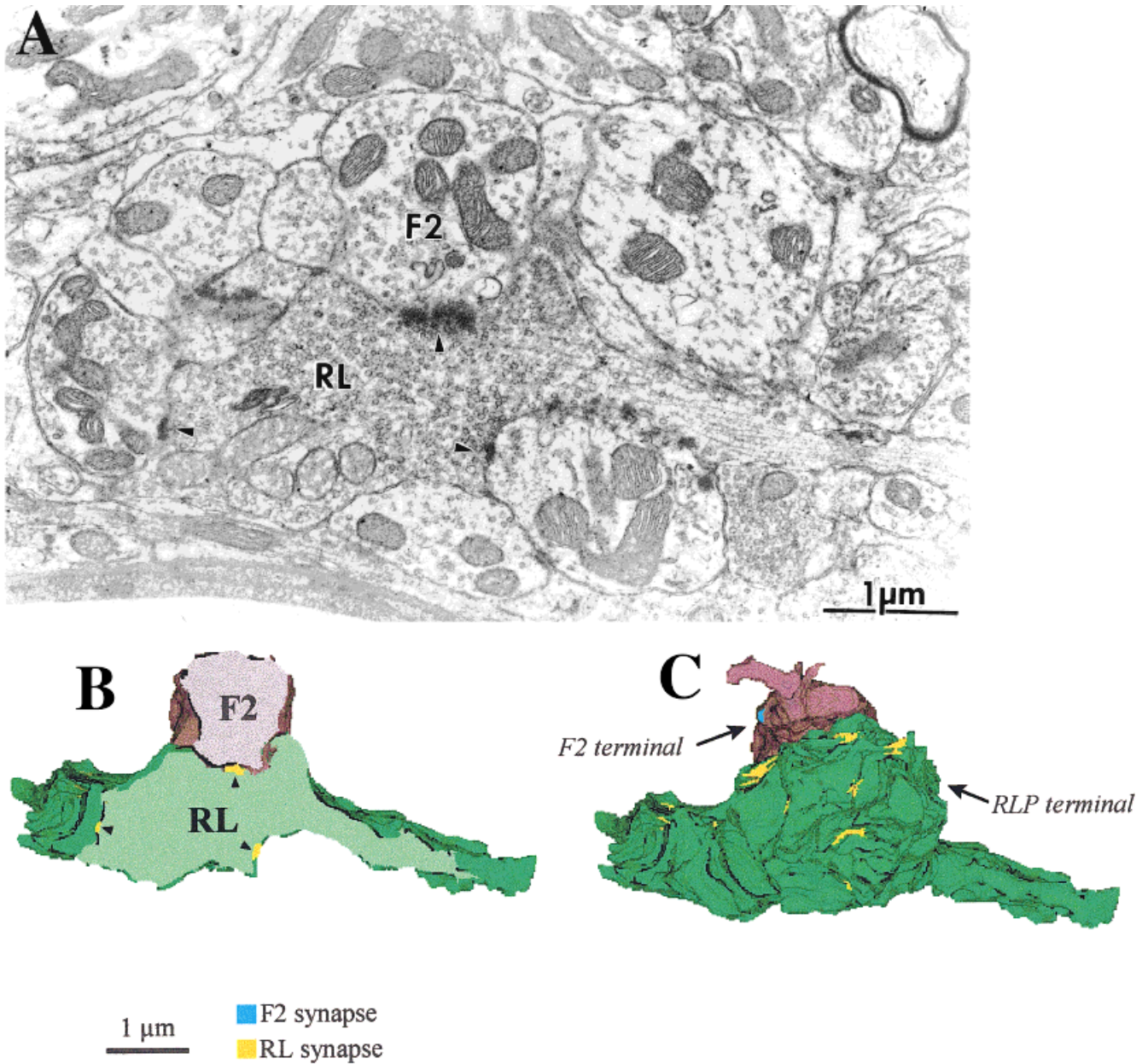


Fig. 2. Example of serial reconstruction for an F2 and RL terminal. **A:** One of the single thin sections of the series, showing an F2 and RL terminal. Three synapses from the RL terminal are indicated by arrowheads, the top one onto the F2 terminal and the others onto

dendrites. **B:** Reconstruction cut through the plane of A (lighter colors). The same three synapses as in A are indicated by the arrowheads. **C:** Complete reconstruction of the F2 and RL terminals with synapses from each shown.

reached a predetermined number (i.e., equal to the number of RS synapses we sampled onto relay cells; see also below). We do not contend that our original sample was unbiased, and in fact we argue that larger synapses are more likely to be sampled. From the serial reconstructions we could determine synaptic sizes and correct for this sampling error. The major assumption we must make is that each of the synaptic types we analyze (RL, RS, F1, and F2) have a synaptic size distribution in our randomly chosen regions of the A-laminae that is representative of the sizes elsewhere in the A-laminae. Nowhere must we assume that the numbers of synapses we sampled are representative or even random.

This is the whole point of correcting for size—we only need assume that the sizes, and not numbers, of the original sample are representative.

The choice of the number of synaptic zones rather than the real measure (e.g., nm) as the unit of synapse size was arbitrary, although the real size of a synaptic zone can potentially be estimated by taking into account such factors as the average thickness of each section (i.e., roughly 80 nm) and shrinkage due to fixation (unmeasured). Figure 5 summarizes the sizes of each synaptic type. Overall, RL terminals formed the largest synaptic zones (traversing 8.8 ± 0.5 sections, $n = 208$), F terminals were next (traversing $6.1 \pm$

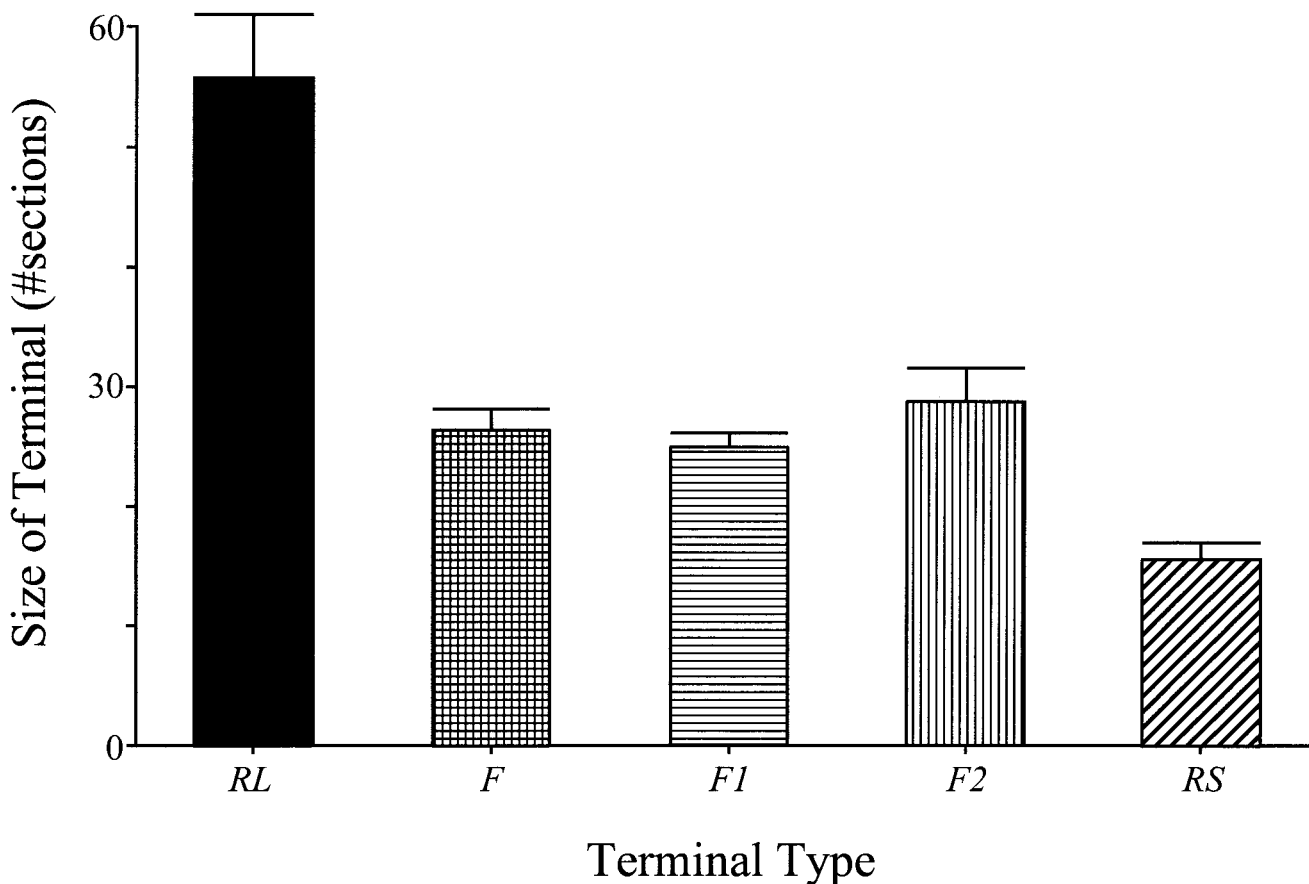


Fig. 3. Mean and standard error of size of each terminal type in the A-laminae of the cat's lateral geniculate nucleus. The size is measured in terms of the number of consecutive thin sections each spans.

0.4 sections, $n = 120$), and contacts from RS terminals were smallest (traversing 5.0 ± 0.2 sections, $n = 159$). Statistically, RL synapses were larger than F ($P < 0.01$) or RS ($P < 0.001$) synapses, but F and RS synapses were not significantly different ($P > 0.1$). However, other differences became manifest whenever it was possible to divide the F terminals into F1 and F2. Synapses from the former (7.0 ± 0.4 sections) were larger than those from the latter (4.1 ± 0.4 sections; $P < 0.001$). Compared with RL synapses, those from F1 terminals were similar in size ($P > 0.1$), but those from F2 terminals were smaller ($P < 0.001$); compared WITH RS synapses, those from F1 terminals were larger ($P < 0.001$), but those from F2 terminals were smaller ($P < 0.001$).

In a subset of our sampled terminals, it was possible to identify the postsynaptic sites as from relay cells or interneurons. There were further differences in synaptic zone size depending on the target or location of each terminal type. For relay cells (Fig. 5B), RL synapses extend over 12.1 ± 0.8 ($n = 111$) sections, which is larger than those from F terminals (5.7 ± 0.4 sections, $n = 42$), including the F1 and F2 subtypes (7.1 ± 0.6 and 4.1 ± 0.4 sections, respectively), and from RS terminals (5.7 ± 0.4 sections, $n = 31$). These differences are statistically significant ($P < 0.001$ for each pairwise comparison for RL terminals). The fact that RL terminals span more sections, on average, than any other type implies that most sampling strategies result in their over-representation. The size differences between F1 and F2 synapses on relay cells and also be-

tween F2 and RS synapses are also significant ($P < 0.001$ for each comparison). However, there is no size difference between RS and F or F1 synapses on relay cells ($P > 0.1$).

On interneurons, the comparison of synaptic sizes shows some surprising differences from those on relay cells (Fig. 5C). Here, RL synapses are the smallest (4.7 ± 0.3 sections, $n = 85$). F terminals are intermediate in size (6.7 ± 0.7 sections, $n = 32$; since no F2 terminals were found in contact with interneurons in our data, these F terminals contacting interneurons are all F1); and RS terminals are the largest (7.2 ± 0.4 sections, $n = 31$). These differences are all statistically significant ($P < 0.01$ for each pairwise comparison for RL terminals). Thus, unlike the situation for relay cells, RL terminals would be under-represented in most sampling strategies.²

² Although it may seem odd that our subset of synapses from RS terminals contacting identified relay cells or interneurons seems larger than our overall, parent sample of RS terminals, in our original sample, this is a nonsignificant variation ($P > 0.05$). It reflects the fact that, as noted above, our initial sample of the subset included only seven RS terminals with synapses onto interneurons, and these were relatively large. We felt that this was too small a sample to provide reliable statistical analysis, and so we performed a second sampling limited to 24 RS synapses onto interneurons. This second sample is valid for establishing the sizes of these synapses, but we did not use it for our estimate of overall RS synaptic sizes because it was biased for this one type of synapse; for the overall RS sample, we used the 159 RS synapses in our original distribution.

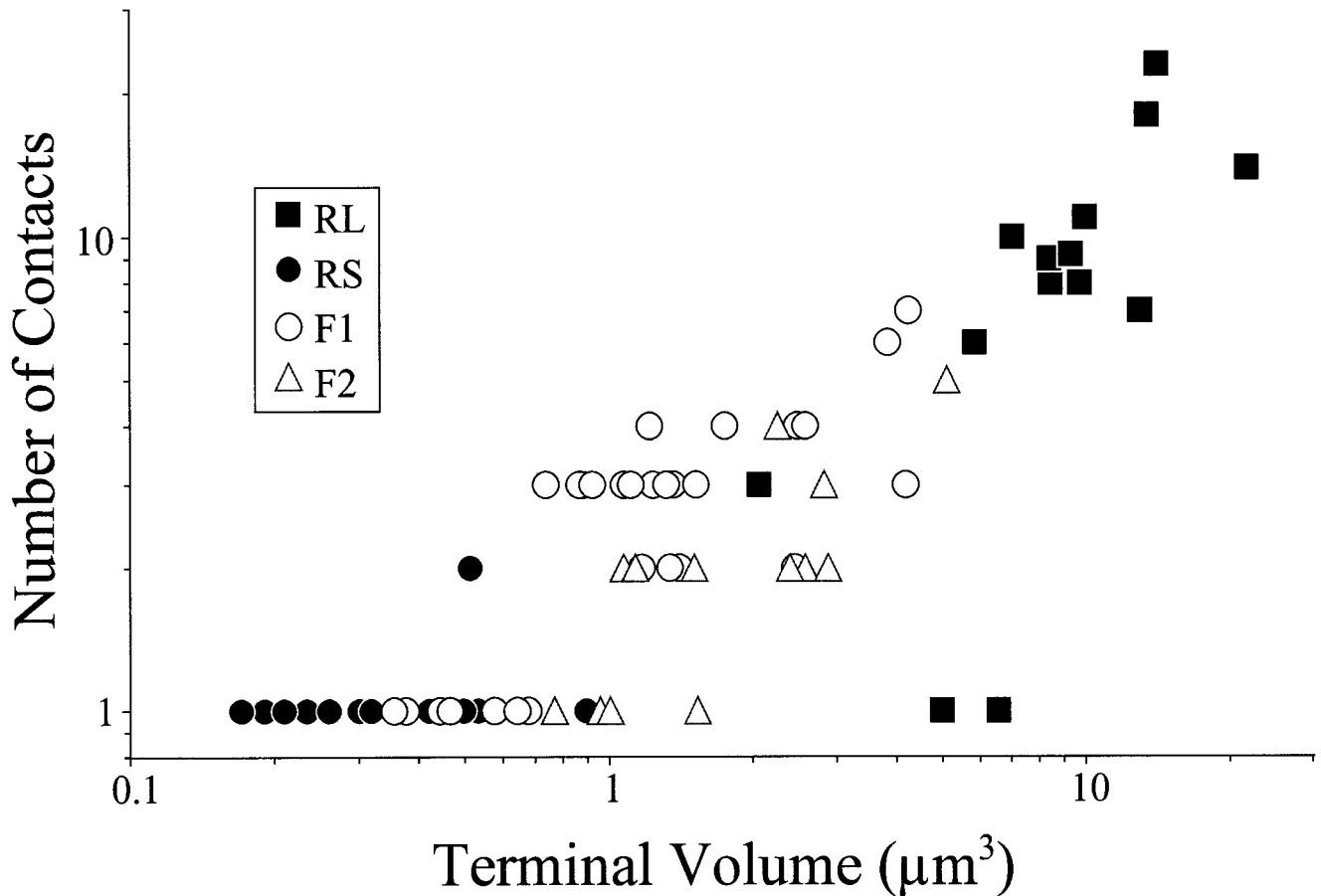


Fig. 4. Sizes of various terminal types from serial reconstructions. Note that there is no overlap in the distributions of the smaller RS and larger RL terminals.

As implied from the above, some of these terminal types differ in the sizes of the synapses they form on relay cells versus interneurons. The differences for RL and RS terminals are statistically significant ($P < 0.001$ and $P < 0.01$, respectively). However, no significant difference was found for F terminals ($P > 0.05$) or their F1 subtype ($P > 0.1$). Also, RL terminals formed larger synapses onto relay cells outside than inside of the glomerular zones (10.2 ± 0.7 sections inside versus 21.5 ± 2.9 sections outside; $P < 0.001$; not illustrated). The situation for RL terminals is different for interneurons (4.47 ± 0.2 sections inside glomeruli and 6.7 ± 1.5 sections outside), but this difference is not significant ($P > 0.1$).

Correction for sampling biases

Number of synapses. We previously reported the relative distribution of synapses from the various terminal types in the geniculate laminae using data collected from single sections (Erişir et al., 1998). That study, based on 1159 synapses from six brains, found that 17.9% of all synapses are formed by RL terminals, 29.3% by F, and 52.9% by RS (Fig. 6A). Because these data were obtained in the traditional manner from single sections, from which it is usually impossible to distinguish between F1 and F2 terminals (i.e., serial reconstruction is required for this distinction), only F terminals as a whole are considered here. Further

analysis of these data revealed the specific distribution pattern of terminals onto relay cells ($n = 994$) and interneurons ($n = 165$) separately: for relay cells, 14.6% of the synapses derive from RL terminals, 29.6% from F, and 55.8% from RS (Fig. 6B); for interneurons, the values are 37.8% from RL terminals, 26.8% from F, and 35.4% from RS (Fig. 6C).

However, as noted in the Introduction, these data and others like them were not corrected for sampling biases based on the greater likelihood of sampling terminals with larger synaptic zones in single thin sections. Our goal here was to provide a correction for a possible bias in many published accounts of terminal distribution that favors sampling terminals with larger synaptic contact zones (see Erişir et al., 1997, for a fuller discussion of this). That is, prior investigators (including us) would select all terminals forming a clear synaptic contact in a proscribed region of a single thin section. Here, we make the assumption that the chance of detecting a terminal with this strategy is linearly proportional to the size of its contact zone (i.e., the larger the contact, the more thin sections it traverses, and the more likely that any single section will capture the contact). We could then estimate the relative probability of sampling each terminal type based on the synaptic zone size, which we have determined in Figure 5. Because we sectioned the material studied here in the same sagittal plane and sampled from similar regions of

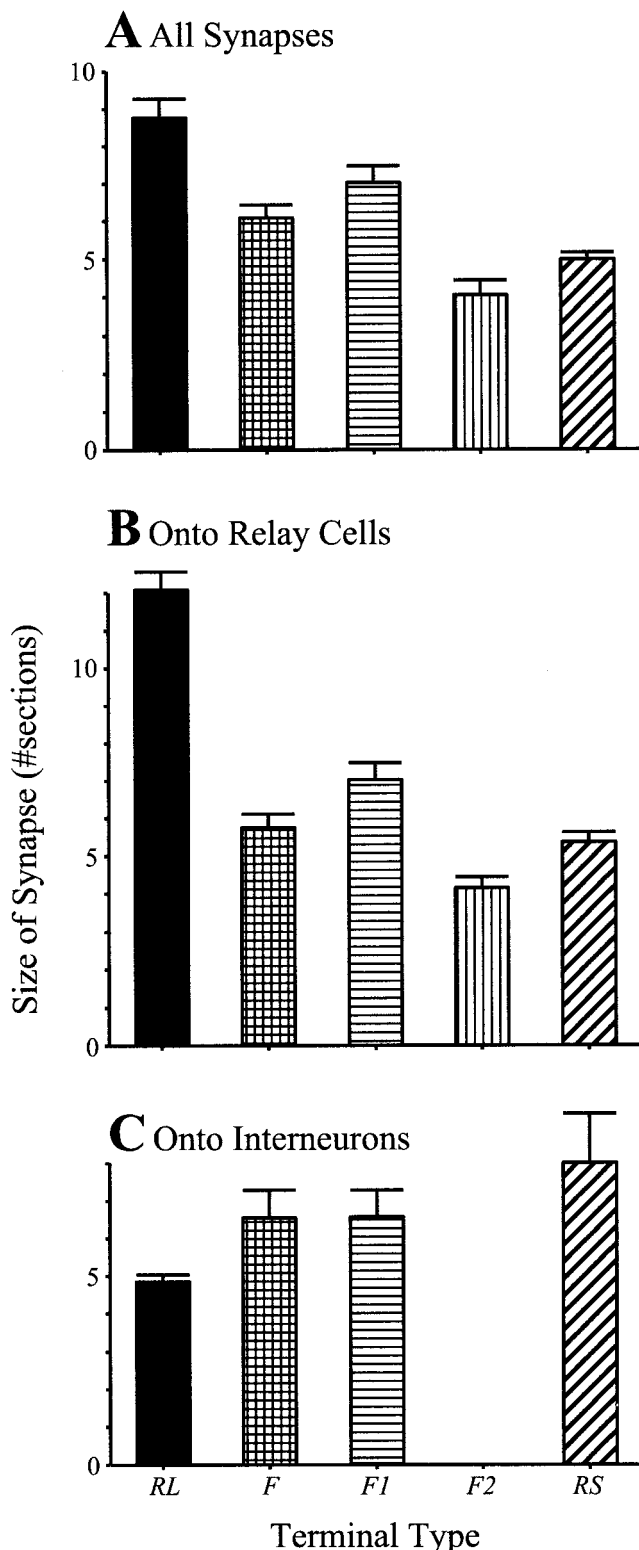


Fig. 5. **A-C**: Mean and standard error of size of synaptic zone formed from each terminal type in the A-laminae of the cat's lateral geniculate nucleus. The size is measured in terms of the number of consecutive thin sections each spans.

the lateral geniculate nucleus, any sampling artifacts based on different anisometries in the shape of synaptic zones from different terminals could be ignored. We could thus reduce the relative probability of encountering one of these terminals to the number of sections in a series that contained the synaptic zone. We can now use this to determine the appropriate correction and apply this to the counts of Figure 6 to obtain a more accurate measure of the relative numbers of the various synaptic types in the neuropil of the lateral geniculate nucleus.

Details of the method we used to correct for sampling biases can be found in Erişir et al. (1997). Briefly, we assumed that the bias of sampling each synaptic type is proportional to its size, or more precisely, to the average number of consecutive sections it spans. We thus adjusted the relative number of each synaptic type accordingly by using two sets of data to estimate the corrected percentages of the various synaptic types, which we denoted *RLs*, *Fs* (or *F1s* and *F2s*), and *RSs*. One set was the raw (uncorrected) percentages of RL, F, and RS synapses (*RLr*, *Fr*, and *RSr*), and the other was the correction factors (number of sections per synapse) for sampling biases of RL, F, and RS synapses (*cRLs*, *cFs*, and *cRSs*). The formulae we adopted were:

RLs =

$$\frac{100 * RLr * cFs * cRSs}{(RLr * cFs * cRSs + cRLs * Fr * cRSs + cRLs * cFs * RSr)} \quad (1)$$

Fs =

$$\frac{100 * Fr * cRSs * cRLs}{(RLr * cFs * cRSs + cRLs * Fr * cRSs + cRLs * cFs * RSr)} \quad (2)$$

RSs =

$$\frac{100 * RSr * cFs * cRLs}{(RLr * cFs * cRSs + cRLs * Fr * cRSs + cRLs * cFs * RSr)} \quad (3)$$

When we applied these corrections to the data of Figure 6A-C, we obtained the following quantitative distribution of geniculate synapses that should now be less affected by sampling biases. Out of all synapses, 11.7% were formed by RL terminals, 27.5% by F, and 60.8% by RS (Fig. 6D). The corrected distribution of synapses onto relay cells revealed that 7.1% came from RL terminals, 30.9% from F terminals, and 62.0% from RS (Fig. 6E).³ Onto interneurons, the values are 47.4% from RL terminals, 23.6% from F, and 29.0% from RS (Fig. 6F). For all three sets of data (i.e., all synapses, those onto relay cells, and those onto interneurons), the difference between the uncorrected and corrected values are statistically significant ($P < 0.001$). Also, in the corrected distributions, the difference in synaptic distributions onto relay cells versus interneurons is statistically significant ($P < 0.001$). Thus, in relative

³ It should be noted that the A-laminae of the cat's lateral geniculate nucleus contains two classes of relay cell, X and Y (reviewed in Sherman and Spear, 1982; Stone, 1983; Sherman, 1985), but our methods did not allow us to distinguish these. Thus our estimates of inputs to relay cells as a group may differ somewhat from the actual values for each class.

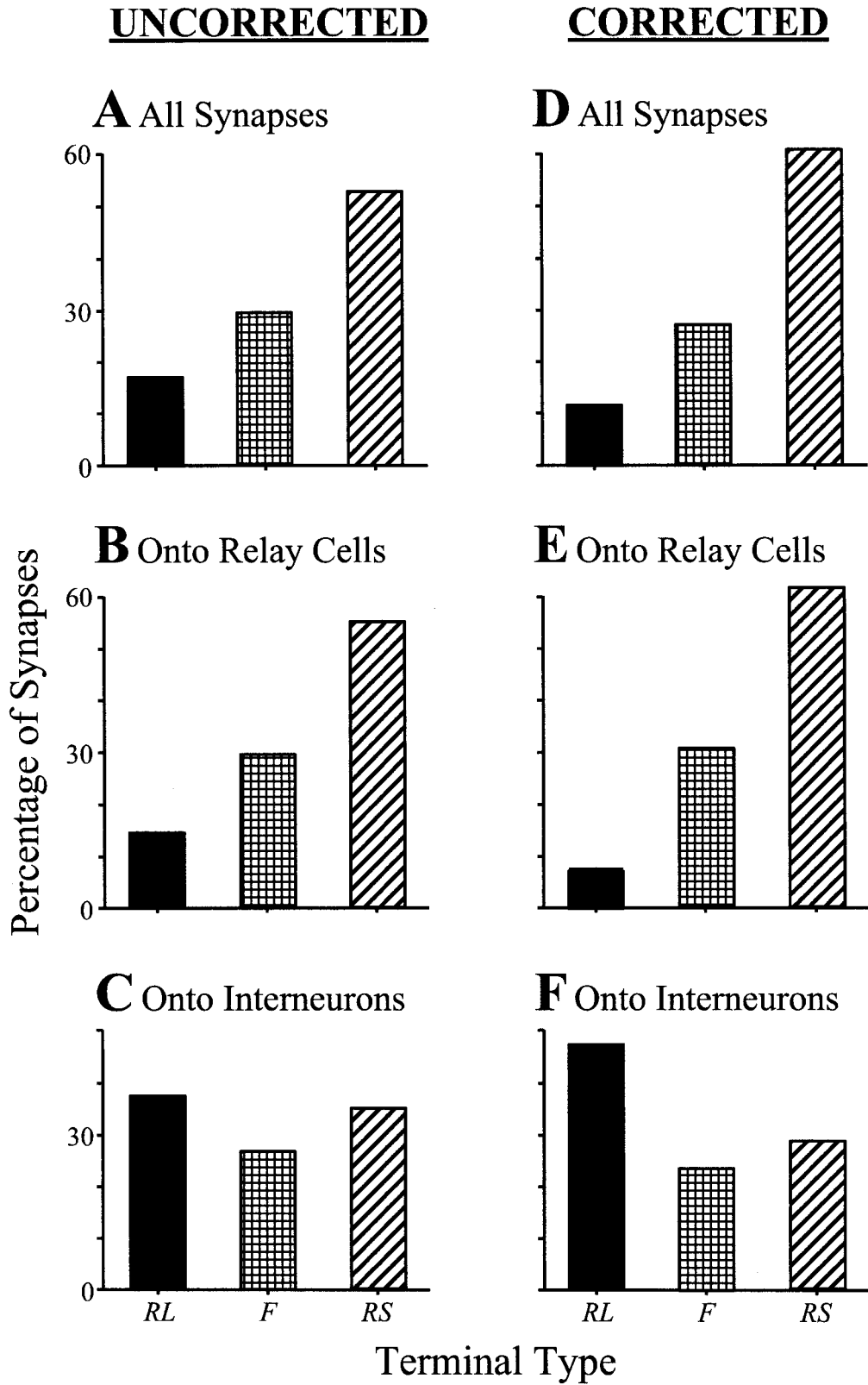


Fig. 6. Percentage of synapses from the three main terminal types in the A-laminae of the cat's lateral geniculate nucleus. **A-C**: Uncorrected percentages, showing synapses for all terminals in the neuropil (A), for contacts onto relay cells (B), and for contacts onto interneurons (C). This is redrawn from Erişir et al., 1998. **D-F**: Corrected percentages for the values of A-C. The corrections were made by using the data from Figure 6 to compensate for oversampling of larger synaptic zones. See text for details.

rons (C). This is redrawn from Erişir et al., 1998. **D-F**: Corrected percentages for the values of A-C. The corrections were made by using the data from Figure 6 to compensate for oversampling of larger synaptic zones. See text for details.

terms, there are many fewer RL synapses and many more RS synapses and somewhat more F synapses on relay cells than on interneurons.

Number of terminals. The above calculations are based on synapse counts, since the sampling starts with an identifiable synapse. However, since synaptic terminals can produce multiple synapses, the relative distribution of actual terminals in the neuropil of the A-laminae cannot be determined just from the corrected estimates of synapse numbers in Figure 6D. For instance, since RL terminals produce many more synapses, on average, than F or RS terminals, the actual relative percentage of retinal terminals in the neuropil is much less than the 11.7% value computed for the relative number of RL synapses. We can use the data of Figure 6D together with those shown in Figure 4 to compute estimates for the terminal distributions. The approach is similar to that described in Eqs. [1]–[3]:

$RLt =$

$$\frac{100 * RLs * cFt * cRSt}{(RLs * cFt * cRSt + cRLt * Fs * cRSt + cRLt * cFt * RSs)} \quad (4)$$

$Ft =$

$$\frac{100 * Fs * cRLt * cRSt}{(RLs * cFt * cRSt + cRLt * Fs * cRSt + cRLt * cFt * RSs)} \quad (5)$$

$RSt =$

$$\frac{100 * RSs * cRLt * cFt}{(RLs * cFt * cRSt + cRLt * Fs * cRSt + cRLt * cFt * RSs)} \quad (6)$$

where: RLt , Ft , and RSt are the estimated percentages of RL, F, and RS terminals; RLs , Fs , and RSs are the corrected percentages of RL, F, and RS synapses (from Eqs. [1]–[3]); and $cRLt$, cFt , and $cRSt$ are the correction factors (number of synaptic zones per terminals) for RL, F, and RS terminals.

Figure 7 shows the results of these calculations. We now estimate that RL terminals represent only 1.8% of all terminals in the A-laminae, F terminals represent 14.5%, and RS terminals represent 83.7%. The rarity of RL terminals has perhaps been unappreciated because of their very large size, which enhances the probability that they will be seen in a given thin section.

DISCUSSION

We have devised a method of controlling for biases in sampling synaptic terminals from single thin sections with the electron microscope. We did this by determining from serial sections the actual size of a synaptic zone, since the probability of encountering a synapse in a single section varies with this size. We applied this to identified synaptic terminals in the A-laminae of the cat's lateral geniculate nucleus and found that the correction for sampling biases produced some changes in previous estimates for the relative numbers of synaptic inputs onto geniculate cells. For instance, we found that retinal terminals were

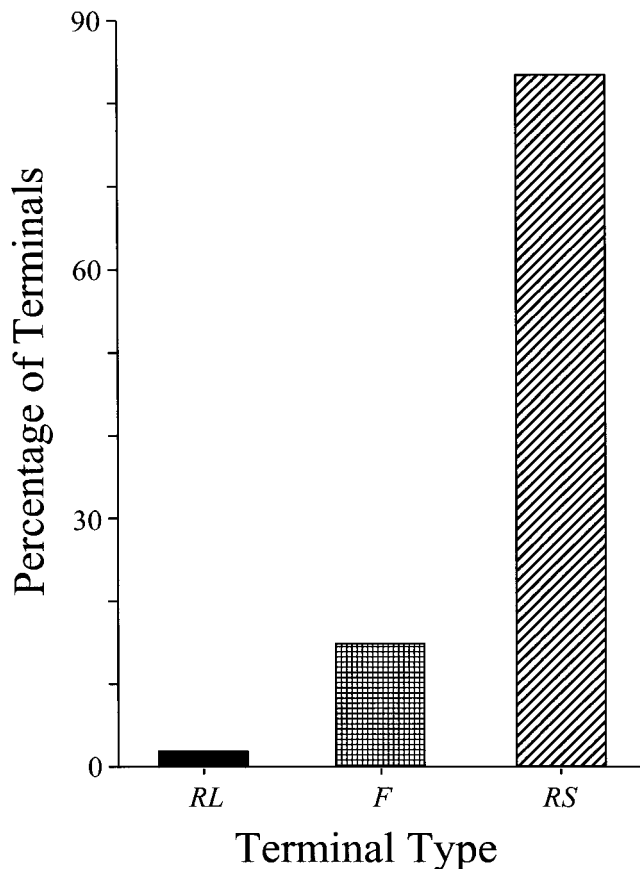


Fig. 7. Percentage of synaptic terminals from the three main terminal types in the A-laminae of the cat's lateral geniculate nucleus. From the data of Figures 4 and 6D–F, we were able to derive these estimates. See text for details.

fewer than previously thought onto relay cells, but somewhat more than previously thought onto interneurons. Although we have restricted our sampling to the lateral geniculate in this study, it would seem possible that this sampling strategy and correction could be used throughout the brain when there is a chance of sampling bias.

Relative numbers of synapses

It had been appreciated for some time that retinal (RL) synapses were a minority of those found in the neuropil, but previous estimates generally placed the value for these to be about 15–20% of all those present. By controlling for sampling biases and also by using immunohistochemistry to determine the relay cell or interneuron targets of these terminals, we now provide new estimates that significantly alter the picture of relative synaptic numbers in the lateral geniculate nucleus. We find that only about 7% of synapses on relay cells are from retina, whereas nearly half of the synapses on interneurons derive from retina. Thus retinal inputs to relay cells are less than half the amount previously suggested, and those on interneurons are twice previously suggested values. It would be useful to know how generally these numbers apply to other thalamic nuclei, but such data are presently unavailable.

Geniculate relay cells receive most of their retinal input from one or a very small number of retinal axons, and the receptive fields of relay cells with their center/surround organization are, to a first approximation, nearly identical to those of their retinal inputs (reviewed in Sherman and Spear, 1982; Stone, 1983; Sherman, 1985). Geniculate receptive fields do not seem very similar to those of their cortical inputs, which do not have a center/surround organization and display selectivity for orientation and often for direction (Tsumoto and Suda, 1980; Grieve and Sillito, 1995). Also, whereas we know little about the response properties of brainstem inputs to the lateral geniculate nucleus, it seems a safe bet that they do not have center/surround receptive fields. It thus seems from a receptive field standpoint that retinal input dominates the response properties of relay cells. This can also be seen in experiments in which a retinal axon and its postsynaptic geniculate target are simultaneously recorded (Cleland et al., 1971; Cleland and Lee, 1985; Usrey et al., 1998), because a large fraction of the action potentials in the geniculate cell are directly attributable to retinal firing.

This picture of retinal input dominating geniculate relay cell properties may at first seem at odds with the observation that retinal synapses are such a small percentage of inputs to these geniculate cells. We can assume that the strength or efficacy of retinal synapses is much stronger, on average, than that of other synapses on relay cells. There are two possible explanations for this. First, this may be related to the finding that the sizes of the retinal contact zones on relay cells tend to be much larger than those of other inputs (Fig. 6). Second, numerous studies have shown that synapses can vary greatly with respect to the probability that an action potential invading the presynaptic terminal will lead to transmitter release (reviewed in Lisman, 1997). If each retinal synapse, on average has a much higher probability of release than other synapses, then the effective excitatory postsynaptic potential (EPSP) from an action potential in a retinal axon would be relatively much larger than expected from the data of Figure 7D–F. For example, if a retinal axon produced, say, 500 synapses on a relay cell, each with a probability of release of 0.9, then an action potential along that axon would lead to 450 active synapses. If several cortical axons together produced 1,000 synapses onto the same cell and fired together, but the probability of release of their synapses was only 0.1, then only 100 synapses would be activated. Thus, before we can begin to relate relative synaptic numbers, as derived in this study, to functional properties, we must know more about synaptic physiology of these inputs than we do presently.

Drivers versus modulators

It has been argued elsewhere (Sherman and Guillery, 1998) that driver and modulator inputs may be generally recognized and distinguished throughout thalamus and perhaps in other parts of the brain and that driver inputs are generally a small minority. By the criteria suggested (Sherman and Guillery, 1998) retinal afferents to the lateral geniculate nucleus can be recognized as the driver input, whereas all the other inputs, from cortex, brainstem, and local GABAergic cells, represent the modulator inputs. In this context of drivers and modulators, we can offer a reasonable but speculative explanation for the observed differences in numbers. To carry basic information to the thalamic target, which is the main purpose of a

driver, requires a relatively small number of inputs. That is not to say that a small number of inputs means a weak postsynaptic effect, because as noted above, driver inputs may have relatively effective synapses. On the other hand, neuromodulation is usually finely graded and may be linked in complicated ways to the many different qualities of behavioral state, such as alertness and attention. Thus to carry out neuromodulatory functions may require a much larger number of inputs. We can also make an analogy to what is seen in many parts of the brain for which the main result of complex neural computations is carried by relatively few cells. In cortex, for instance, the number of cells carrying the output message for a column (e.g., some layer 5 cells projecting to subcortical targets) represents a minority of cells in the column.

It is also interesting to compare, in cats, the retinogeniculate inputs with geniculocortical inputs to layer 4 of striate cortex. Both inputs can be recognized as drivers, because both determine the basic receptive field properties of their postsynaptic cells (Cleland and Lee, 1985; Ferster, 1987, 1994; Reid and Alonso, 1996; Usrey et al., 1998). It has been estimated that geniculocortical axons contribute only about 5–6% of the total synapses to their target cells in layer 4 (Peters and Payne, 1993; Ahmed et al., 1994). This value is remarkably close to the 7% we have determined for retinal input to geniculate relay cells. Perhaps this close quantitative similarity for two different driver pathways is a coincidence, but we can only determine how commonly driver inputs are limited to 5–10% of synapses at their target by quantitatively studying more identified driver pathways.

CONCLUSIONS

We have determined with methods that control for problematic sampling biases that retinal inputs to relay cells in the lateral geniculate nucleus of the cat produce only 7% of the synapses on these cells, although they produce nearly half the inputs to interneurons. However, for relay cells that must transport retinal messages to cortex, most inputs derive from cortex, brainstem, and local GABAergic cells. One important conclusion we draw from this is that it can often be greatly misleading to attribute relative functional importance to relative numbers of synapses. For instance, if we had only the sort of anatomical information about the lateral geniculate nucleus provided in the current study, we might be tempted to conclude that this nucleus was little influenced by retina and instead mainly relayed brainstem information to cortex. This caution may apply outside of thalamus as well. Thus, until one knows the functional significance of a pathway, particularly with regard to its driver or modulator status, one would be unwise to attribute much functional significance to that pathway.

LITERATURE CITED

- Ahmed B, Anderson JC, Douglas RJ, Martin KAC, Nelson JC. 1994. Polynuclear innervation of spiny stellate neurons in cat visual cortex. *J Comp Neurol* 341:39–49.
- Bickford ME, Günlük AE, Van Horn SC, Sherman SM. 1994. GABAergic projection from the basal forebrain to the visual sector of the thalamic reticular nucleus in the cat. *J Comp Neurol* 348:481–510.
- Bickford ME, Günlük AE, Guido W, Sherman SM. 1993. Evidence that cholinergic axons from the parabrachial region of the brainstem are the exclusive source of nitric oxide in the lateral geniculate nucleus of the cat. *J Comp Neurol* 334:410–430.

- Cleland BG, Lee BB. 1985. A comparison of visual responses of cat lateral geniculate nucleus neurones with those of ganglion cells afferent to them. *J Physiol (Lond)* 369:249–268.
- Cleland BG, Dubin MW, Levick WR. 1971. Sustained and transient neurones in the cat's retina and lateral geniculate nucleus. *J Physiol (Lond)* 217:473–496.
- Erişir A, Van Horn SC, Sherman SM. 1997. Relative numbers of cortical and brainstem inputs to the lateral geniculate nucleus. *Proc Natl Acad Sci USA* 94:1517–1520.
- Erişir A, Van Horn SC, Sherman SM. 1998. Distribution of synapses in the lateral geniculate nucleus of the cat: differences between laminae A and A1 and between relay cells and interneurons. *J Comp Neurol* 390:247–255.
- Ferster D. 1987. Origin of orientation-selective EPSPs in simple cells of cat visual cortex. *J Neurosci* 7:1780–1791.
- Ferster D. 1994. Linearity of synaptic interactions in the assembly of receptive fields in cat visual cortex. *Curr Opin Neurobiol* 4:563–568.
- Grieve KL, Sillito AM. 1995. Differential properties of cells in the feline primary visual cortex providing the corticofugal feedback to the lateral geniculate nucleus and visual claustrum. *J Neurosci* 15:4868–4874.
- Guillery RW. 1969a. A quantitative study of synaptic interconnections in the dorsal lateral geniculate nucleus of the cat. *Z Zellforsch* 96:39–48.
- Guillery RW. 1969b. The organization of synaptic interconnections in the laminae of the dorsal lateral geniculate nucleus of the cat. *Z Zellforsch* 96:1–38.
- Lisman JE. 1997. Bursts as a unit of neural information: making unreliable synapses reliable. *Trends Neurosci* 20:38–43.
- Montero VM. 1991. A quantitative study of synaptic contacts on interneurons and relay cells of the cat lateral geniculate nucleus. *Exp Brain Res* 86:257–270.
- Peters A, Payne BR. 1993. Numerical relationships between geniculocortical afferents and pyramidal cell modules in cat primary visual cortex. *Cereb Cortex* 3:69–78.
- Phend KD, Weinberg RJ, Rustioni A. 1992. Techniques to optimize post-embedding single and double staining for amino acid neurotransmitters. *J Histochem Cytochem* 40:1011–1020.
- Reid RC, Alonso JM. 1996. The processing and encoding of information in the visual cortex. *Curr Opin Neurobiol* 6:475–480.
- Sherman SM. 1985. Functional organization of the W-, X-, and Y-cell pathways in the cat: a review and hypothesis. In: Sprague JM, Epstein AN, editors. *Progress in psychobiology and physiological psychology*, vol 11. Orlando: Academic Press. p 233–314.
- Sherman SM, Guillery RW. 1996. The functional organization of thalamo-cortical relays. *J Neurophysiol* 76:1367–1395.
- Sherman SM, Guillery RW. 1998. On the actions that one nerve cell can have on another: Distinguishing “drivers” from “modulators.” *Proc Natl Acad Sci USA* 95:7121–7126.
- Sherman SM, Koch C. 1998. Thalamus. In: Shepherd GM, editor. *The synaptic organization of the brain*, 3rd ed. New York: Oxford University Press. p 289–328.
- Sherman SM, Spear PD. 1982. Organization of visual pathways in normal and visually deprived cats. *Physiol Rev* 62:738–855.
- Stone J. 1983. *Parallel processing in the visual system*. New York: Plenum Press.
- Tsumoto T, Suda K. 1980. Three groups of cortico-geniculate neurons and their distribution in binocular and monocular segments of cat striate cortex. *J Comp Neurol* 193:223–236.
- Usrey WM, Reppas JB, Reid RC. 1998. Paired-spike interactions and synaptic efficacy of retinal inputs to the thalamus. *Nature* 395:384–387.
- Wilson JR, Friedlander MJ, Sherman SM. 1984. Fine structural morphology of identified X- and Y-cells in the cat's lateral geniculate nucleus. *Proc R Soc Lond B* 221:411–436.